Query Details

Back to Main Page

1. Please check if the section headings are assigned to appropriate levels.

OK

2. Please check and confirm "Sabelli and Zanazzi (Acta Cryst B24:1214-1221, 1968)" if captured correctly and amend as necessary.

OK

3. The citation Sabelli and Zanazzi (1986) has been changed into Sabelli and Zanazzi (1968) to match the author name/date in the reference list. Please check here and in subsequent occurrences, and correct if necessary.

OK

4. Reference ShelxL (2014) was mentioned in the manuscript; however, this was not included in the reference list. As a rule, all mentioned references should be present in the reference list. Please provide the reference details to be inserted in the reference list and ensure that all references are cited in ascending numerical order

The correct reference is ShelxL (2015)

5. Please check if data and captions of all tables are presented correctly.

OK

Original Paper

Serpierite polytypoids from Zvezdel, Bulgaria, and Lavrion, Greece

Rositsa P. Nikolova
Email : rosica.pn@clmc.bas.bg
Affiliationids : Aff1, Correspondingaffiliationid : Aff1
Nadia L. Petrova Affiliationids : Aff1
Zlatka G. Delcheva Affiliationids : Aff1
Liliya V. Tsvetanova Affiliationids : Aff1
Tsveta Stanimirova Affiliationids : Aff2
Iskra Piroeva Affiliationids : Aff3

Aff1 Institute of Mineralogy and Crystallography, Bulgarian Academy of Sciences, Acad. G. Bonchev Str. 107, 1113, Sofia, Bulgaria

Aff2 Sofia University “St. Kliment Ohridski”, Faculty of Geology and Geography, Bul. “Tsar Osvoboditel” 15, 1504, Sofia, Bulgaria

Aff3 Institute of Physical Chemistry, Bulgarian Academy of Sciences, Acad. G. Bonchev Str. 11, 1113, Sofia, Bulgaria

Received: 9 March 2022 / Accepted: 20 October 2022

Abstract

Structural characteristics of serpierite samples from Zvezdel, Bulgaria, and Lavrion, Greece, are reported. The thermal behaviour of serpierite from Lavrion is discussed. The chemical composition of the studied samples is analysed by energy-dispersive spectroscopy (EDS) and confirmed by single-crystal structure refinements. The obtained chemical formulas correspond well to that of serpierite with Cu:Zn ratio varying between 2.9 and 5.6. The sample from Zvezdel, with composition $Ca[Cu_{3.3}Zn_{0.7}(OH)_6(SO_4)_2 \bullet 3H_2O$, crystallizes in the monoclinic crystal system, with space group *I*2 and unit-cell parameters $a = 18.418(3)$, $b = 6.220(1)$, $c = 12.091(2)$ Å, $\beta = 90.78(1)^\circ$, whereas the one from Lavrion $Ca[Cu_{2.8}Zn_{1.2}(OH)_6(SO_4)_2] \bullet 3H_2O$, shows similar unit-cell parameters $a = 18.394(1)$, $b = 6.256(1)$, $c = 12.097(1)$ Å, $\beta = 90.92(1)^\circ$, but higher *I2/m* space-group symmetry. Both studied crystals exhibit serpierite structure topology, but different stacking sequence of the octahedral layers. While in previously studied serpierite of Sabelli and Zanazzi (Acta Cryst B24:1214-1221, 1968) there are two layers per unit cell, in currently studied samples there is only one. As a consequence, their unit-cell volumes are half than that of the first structurally characterized serpierite specimen with SG *C*2/*c* and unit-cell parameters $a = 22.186(2)$, $b = 6.250(2)$, $c = 21.853(2)$ Å, $\beta = 113.36(1)^\circ$. Taking into account the structural peculiarities of the studied samples they are considered as serpierite polytypoids.

Keywords

Serpierite
Polytypoid
Crystal structure
Chemical composition
Thermal behaviour

Editorial handling: A. Beran

Supplementary Information

The online version contains supplementary material available at https://doi.org/10.1007/s00710-022-00797-9.

Introduction

AQ1 The mineral serpierite is a calcium-copper-zinc hydroxy-sulfate, formed by exogenous alteration of copper–bearing sulfides. AQ2 It forms greenish-blue flat-shaped to acicular crystals and occurs in the oxidized zones of Cu–Zn deposits e.g. (Matsubara 1973; Takada and Matsuuchi 1981; Yakhontova et al. 1981, 1984; Bridges 1987; Van Tassel 1979; Campostrini and Gramaccioli 2001; Ohnishi et al. 2002, 2004, 2007, 2013; Zaharia 2003; Hammarstrom et al. 2005; Kolitsch et al. 2013). It was first found by Bertrand in the Lavrion mine, Greece and its morphology and optical properties were described by Des Cloizeaux in the same year (Bertrand 1881; Des Cloizeaux 1881). The name “serpierite” was given in honour of Giovanni Battista Serpieri. The chemical composition of serpierite from Lavrion has been first reported in 1895 (Frenzel 1895). Later on single crystal structural analyses were performed by Sabelli and Zanazzi (1968). The reported sample crystallizes in the monoclinic space group *C*2/*c* with unit-cell parameters $a = 22.186(2)$, $b = 6.250(2)$, $c = 21.853(2)$ Å, $\beta = 113.36(1)^\circ$ and chemical formula $Ca(Cu,Zn)_4(SO_4)_2(OH)_6 \bullet 3H_2O$ (Cu:Zn = 1.9). Although in the following decades many authors have reported occurrences of serpierite in different exogenous mineral systems, data on chemical composition and structural parameters are surprisingly rare. It is assumed that the Cu:Zn ratio varies for samples from different localities, but analytical data are reported only for a sample from Trestia-Băiţa, Romania (Cu:Zn = 2.8) (Zaharia 2003) and two samples from Broken Hill, New South Wales, Australia: Cd-serpierite with Cu:Zn = 2 (Elliott and Willis 2010) and aldridgeite with Cu:Zn = 2.6 (Elliott and Pring 2015). The given values of the copper – zinc ratio are based on single crystal data only for Cd-serpierite, while the other two are calculated from electron microprobe analysis. Due to the generally very small size of

serpierite crystals, powder diffraction data were usually used to evaluate the structural parameters. Single-crystal structure refinements were reported only for samples from Lavrion, Broken Hill and the Baccu Locci mine (Elliott and Willis 2010; Elliott and Pring 2015; Campostrini and Gramaccioli 2001). The last one has unit-cell parameters $a = 21.906(2)$, $b = 6.238(2)$, $c = 12.130(2)$ Å, $\beta = 122.69(1)^\circ$ which are significantly different from those reported by Sabelli and Zanazzi (1968). AQ3 Unfortunately, it was not possible to find an announced report regarding the redetermination of the serpierite crystal structure ("Pilati et al. in prep.", announced by Campostrini and Gramaccioli 2001). The mineral serpierite belongs to hydroxy-hydrated copper-sulfate minerals with doubly decorated sheets. The common structural unit of these minerals is a $[M^{2+}\varphi_2]$ (M = metal cation; $\varphi = (SO_4)^{2-}$) sheet decorated on both sides by divalent $(SO_4)^{2-}$ anions (Hawthorne and Schindler 2000). Depending on the chemical composition, the $[M^{2+}\varphi_2]$ sheets can be electro-neutral so the interlayer space accepts H_2O molecules only. In other cases, the sheets are negatively charged and the electro-neutrality of the structure is achieved by additional cations in the interlayer space.

Recently, new data for minerals from the Zvezdel deposit, Bulgaria, were reported (Delcheva et al. 2017). The powder X-ray diffraction (XRD) data and chemical analyses of one of the reported samples indicate that it was most probably copper-rich serpierite with a Cu:Zn ratio of 5.7. In order to compare the serpierite from Zvezdel with that of a reference sample from the type locality (Lavrion, Greece) we have performed a crystal-chemical study of samples from both Zvezdel and Lavrion. The crystal-structure peculiarities of the studied samples are discussed in the context of the structural topologies of other hydroxy-hydrated copper-sulfate minerals.

Experimental

Materials

Samples of serpierite crystals from the Zvezdel deposit (SZ) and Lavrion mining district (SL) were studied. The SZ specimen is from the oxidized zone of an epithermal deposit belonging to the Zvezdel-Pcheloyad ore field (Eastern Rhodopes, Bulgaria). The sample has been donated by Mr. V. Krastev and is deposited in the mineral collection of the Institute of Mineralogy and Crystallography, Bulgarian Academy of Sciences (N 0691). The Zvezdel ore field predominantly consists of veins, hosted in shoshonitic to high—potassium calc-alkaline volcanic rocks and exhibits characteristics of intermediate-sulphidation epithermal Pb–Zn–Cu ± Ag–Au deposit (Marchev et al. 2005; Moritz et al. 2010). The mineral association of studied sample has been reported by Delcheva et al. (2017) and consists of gypsum, dolomite, galena, sphalerite, chalcopyrite, quartz and calcite. The N 0691 specimen includes serpierite, which forms greenish-blue crusts covering tiny gypsum crystals.

The SL sample was kindly provided by the staff of the "Earth and Man" National Museum in Sofia, Bulgaria (cat. no. N 13,291). The N 13,291 specimen contains clusters of very tiny greenish-blue serpierite crystals. The powder samples for XRD and thermal analyses were prepared by mechanical separation of serpierite crystals under an optical microscope. The separation, especially for the Zvezdel sample, was difficult due to the very small size of the serpierite crystals (up to 0.01 mm) which makes them hard to distinguish from accompanying gypsum.

Analytical methods

Scanning electron microscopy (SEM) and energy-dispersive spectroscopy (EDS)

The morphological and chemical analyses of the samples from both deposits were performed on a JSM 6390 electron microscope (Japan) in conjunction with energy dispersive X-ray spectroscopy (EDS, Oxford INCA Energy 350) equipped with ultrahigh resolution scanning system (ASID-3D) at following conditions: 20 kV accelerating voltage, I ~ 75 mA, vacuum medium in the range of 10^{-4} Pa, spot size 1 μm. The sample is mounted on a double coated conductive carbon tape that holds the sample firmly to the stage surface and can be used as a ground strap from the sample surface to sample holder. The samples were gold coated with time of coating ~ 40 s.

Powder X-ray diffraction analyses

About 1 g of pale blue prismatic crystals, presumably serperite, were separated from the bulk for both studied samples. X-ray powder diffraction analyses were performed using Empyrean, Panalytical diffractometer

XRD, 2Θ range 4–70, step 0.01°, 1 s per step, Cu*K*α radiation (λ = 1.54 Å).

Thermal analyses

Differential scanning calorimetry (DSC) and thermogravimetry (TG) were carried out using an SETSYS2400 Evolution, (SETARAM) apparatus at the following conditions: temperature range from 20 to 1000 °C, static air atmosphere, heating rate of 10 °C min^{-1}, and 10–15 mg sample mass in corundum crucibles. Simultaneous analysis of the evolved gases was performed via mass spectrometry (MS) using an OmniStar mass spectrometer connected to the TG apparatus. The intensities related to the m/z (mass-to-charge ratio) value of H_2O (18), O_2 (32) and SO_2 (64) were examined.

Single crystal XRD

Prismatic, nearly colourless crystals from SZ and SL were each mounted on a glass capillary and analysed by a single crystal diffraction method using a SuperNova, Dual wavelength (Rigaku) single crystal diffractometer. The data collection and data reduction were performed by CrysAlisPro, Rigaku Oxford Diffraction, 2017, version 1.1.171.37.35 (CrysAlis PRO 2011). Fast scan was performed on three crystals from SL and three from SZ in order to find crystals suitable for data collection experiment. All of the scanned crystals showed a unit-cell volume half than the one reported by Sabelli and Zanazzi (1968). The non-standard monoclinic setting was accepted for both studied samples, because the beta angle in the used *I* centred unit-cell is closer to 90° than that in the standard *C* centred one. The observed diffraction patterns characterize both studied samples as single-phase ones. The crystal structures were solved by direct methods using ShelxS and refined by the full-matrix least-squares method on F^2 with ShelxL ~~(2014)~~ AQ4 programs (Sheldrick 2008, 2015). All of the atom positions were located successfully from difference Fourier maps. The structure determination reveals that both samples are built of $[(Cu,Zn)_4(SO_4)_2(OH)_6]^{2-}$ octahedral layers, calcium ions and H_2O molecules. The Cu and Zn ions were placed on individual or mixed positions depending on the geometry of the corresponding octahedron. For SZ four symmetrically non-equivalent positions for S atoms were located (S11, S12, S21, S22). The S11 – S12 and S21 – S22 distances are shorter than 1 Å, indicating sulfate groups disorder. The contribution of each SO_4 group was refined. In the case of SL two symmetrically independent positions for S atoms were located (S1 and S2). Both S1 and S2 have symmetrically equivalent atoms at a distance of less than 1 Å, so the S1 and S2 positions were refined with occupancy 0.5. The calcium atoms positions, two for SZ and one for SL also indicate disordered arrangement. The refinement of the Ca positions occupancy factors was achieved taking into consideration the geometric features of the structure. It was not possible to locate the hydrogen atoms of H_2O molecules and OH groups so the number of hydrogens in the chemical formula was added to balance the negative charge. The obtained structural models for SZ and SL are optimal with respect to the geometrical restrictions, site occupancy parameters, and reliability factors. The obtained structural models were first refined with isotropic temperature factors. Finally, the anisotropic displacement parameters of all atoms for SL and non-oxygen atoms for SZ were refined. Selected crystal data and structure refinement parameters are listed in Table 1. The fractional atomic coordinates of SL and SZ structures are listed in Tables S1 and S2, respectively. Crystallographic data for their crystal structures are deposited in the Cambridge Crystallographic Data Centre, No. CSD 2155845 (SZ) and No. CSD 2155846 (SL). For the purposes of the following discussion, concerning the similarity of the compounds with serpierite structure topologies, the unit-cells of SZ and SL were transformed to the corresponding standard settings, using the program SETSTRU of Bilbao Crystallographic server (Aroyo et al. 2011). AQ5

Table 1

Most important data collection and refinement parameters for the studied samples

Sample	Zvezdel, Bulgaria (SZ)	Lavreon, Greece (ZL)
Chemical formula	$Ca(Cu_{3.3}Zn_{0.7})(SO_4)_2(OH)_6•3H_2O$	$Ca(Cu_{2.76}Zn_{1.24})(SO_4)_2(OH)_6•3H_2O$
Formula weight	1263.28	1265.23
Temperature	290(2) K	290(2) K

Sample	Zvezdel, Bulgaria (SZ)	Lavreon, Greece (ZL)
Wavelength	0.71073 Å	0.71073 Å
Crystal system	Monoclinic	Monoclinic
Space group	I 2	I 2/m
Unit cell dimensions	a = 18.418(3) Å	a = 18.3942(6) Å
	b = 6.2203(10) Å	b = 6.2562(2) Å
	c = 12.0909(16) Å	c = 12.0967(5) Å
	β = 90.781(13)°	β = 90.923(3)°
Volume	1385.1(4) $Å^3$	1391.88(9) $Å^3$
Z	2	2
Density (calculated)	3.029 mg/m^3	3.019 mg/m^3
Absorption coefficient	6.961 mm^{-1}	14.167 mm^{-1}
F(000)	1219	1221
Crystal size	0.04 × 0.02 × 0.01 mm^3	0.3 × 0.25 × 0.12 mm^3
Theta range for data collection	3.370 to 29.414°	4.343 to 74.446°
Index ranges	$-17 \le h \le 24$, $-8 \le k \le 7$, $-16 \le l \le 13$	$-22 \le h \le 21$, $-5 \le k \le 7$, $-15 \le l \le 15$
Reflections collected	3587	4589
Independent reflections	2681 [R(int) = 0.0547]	1530 [R(int) = 0.0208]
Completeness to theta = 25.242°	99.7%	100.0%
Refinement method	Full-matrix least-squares on F^2	Full-matrix least-squares on F^2
Data / restraints / parameters	2681 / 1 / 168	1530 / 0 / 171
Goodness-of-fit on F^2	0.969	1.052
Final R indices [$I > 2$sigma(I)]	$R1$ = 0.0785, w$R2$ = 0.1323	$R1$ = 0.0341, w$R2$ = 0.0974
R indices (all data)	$R1$ = 0. 2133, w_R2 = 0. 1933	$R1$ = 0.0434, w$R2$ = 0.1059
Absolute structure parameter	0.2(3)	
Weighting scheme	$w = [\sigma^2(Fo^2) + (0.0368P)^2]^{-1}$ where $P = (Fo^2 + 2Fc^2)/3$	$w = [\sigma^2(Fo^2) + (0.0588P)^2 + 2.4961P]^{-1}$ where $P = (Fo^2 + 2Fc^2)/3$
Largest diff. peak and hole	1.185 and -1.019e.$Å^{-3}$	0.839 and -0.507 e.$Å^{-3}$

Results and discussion

Results

Morphological and chemical analyses

Microscopically, under SEM, both samples SZ and SL show thin elongated plate-like crystals with sizes between 50–100 µm (Fig. 1). Results of the SEM–EDS spot analyses are presented in Table S3. The obtained data reveal that in both cases the Cu:Zn ratio varies from crystal to crystal in a relatively wide range and have an average value of 4.025 for the SZ sample and 2.78 for the SL one. The results obtained for SL are comparable with those reported by Sabelli and Zanazzi (1968). Although the chemical analyses show that Cu:Zn ratio varies widely even for crystals from the same locality, it is evident that the studied crystals from Zvezdel, Bulgaria, contain, in average, smaller amount of zinc than the serpierite crystals described until now.

Fig. 1

SEM images of the studied samples **a** SZ and **b** SL

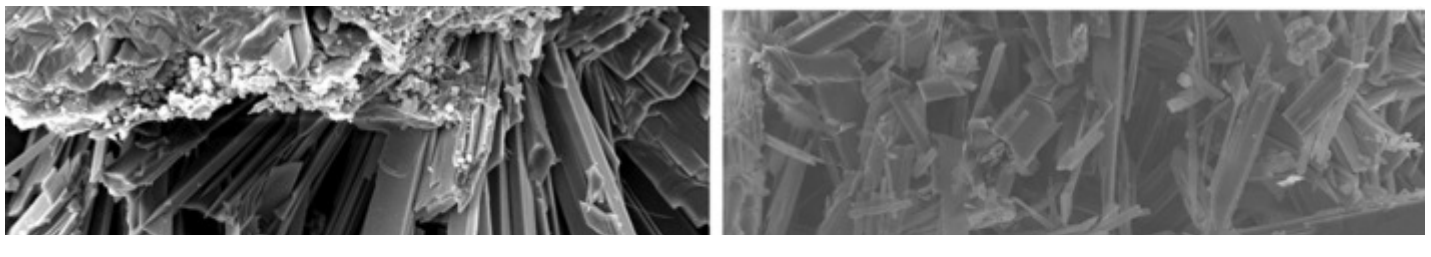

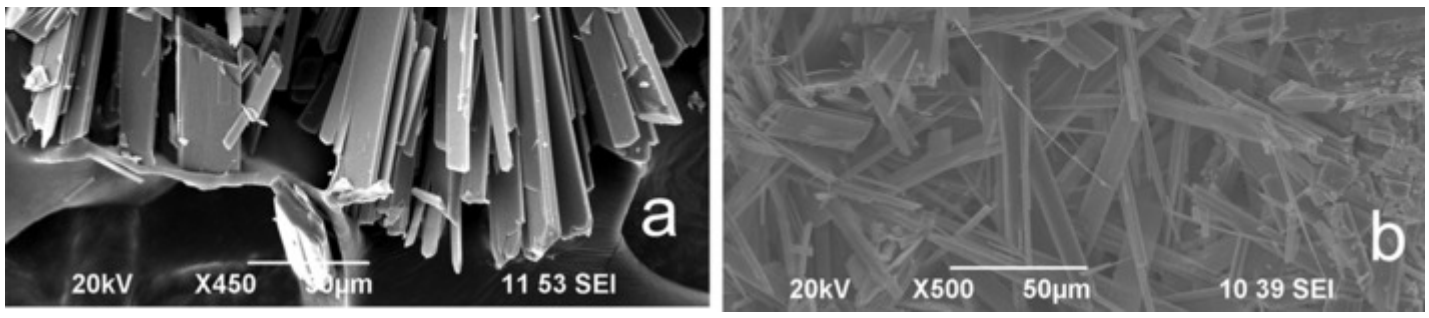

Powder x-ray diffraction analyses

The powder X-ray diffraction data are presented in Fig. 2. Both patterns are affected by the layered character of SL and SZ structures. The SZ powder samples consists of a mixture of serpierite and gypsum. The larger size crystals from the SL allowed the separation of a sufficient amount of almost monomineralic serpierite. The data showed that only the SL powder sample is pure enough to be used for DSC-TG analyses.

Fig. 2

X-ray powder diffraction patterns of the studied samples **a** SZ and **b** SL Serp – serpierite, Gy – gypsum, Qtz – quartz, Cal – calcite

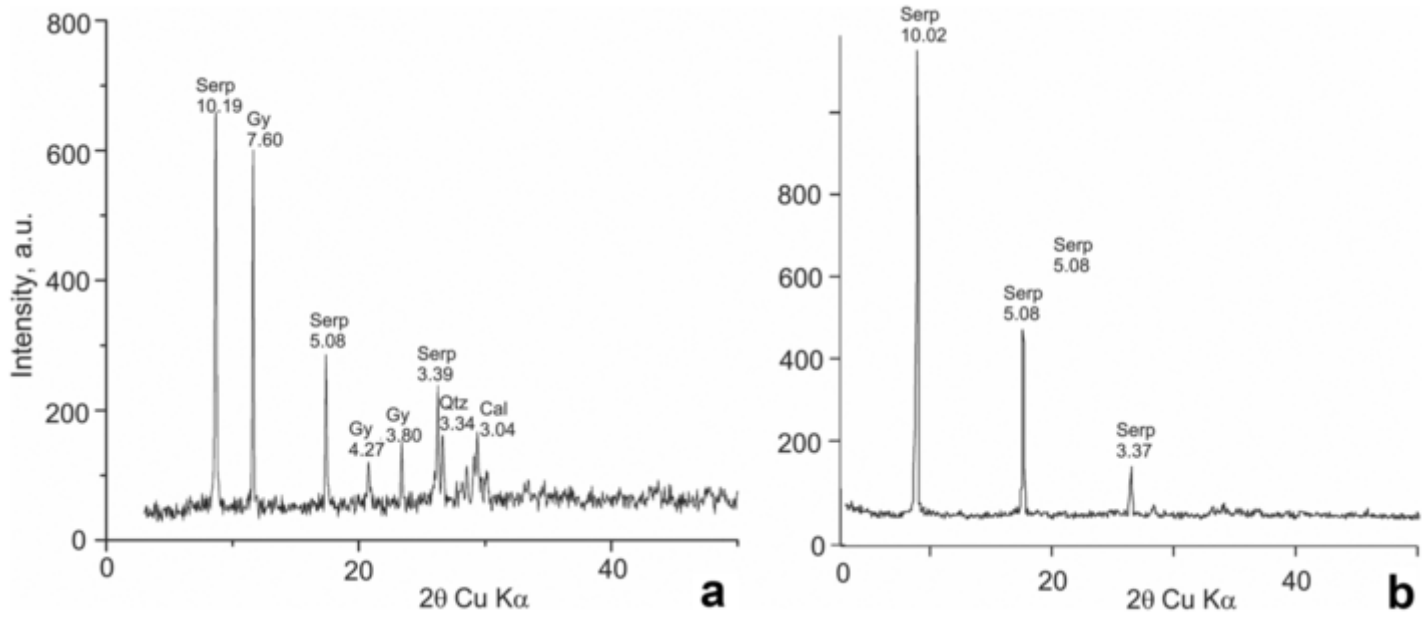

Thermal analyses

DSC-TG(DTG)-MS curves of the SL are presented on Fig. 3 where the endo- and exo- effects are numbered starting from the lowest temperature one. The SL thermal decomposition is characterised as consecutive stages of dehydration, dehydroxylation and SO_4 degradation. Similar behaviour has been observed in DTA-TG(DTG) study of serpierite $(Cu,Ca)_{2.5}(SO_4)(OH)_3 \bullet 1.5H_2O$ from the Komsomol deposit, Eastern Siberia, Russia (Yakhontova et al. 1984).

Fig. 3

DSC-TG(DTG)-MS curves of SL

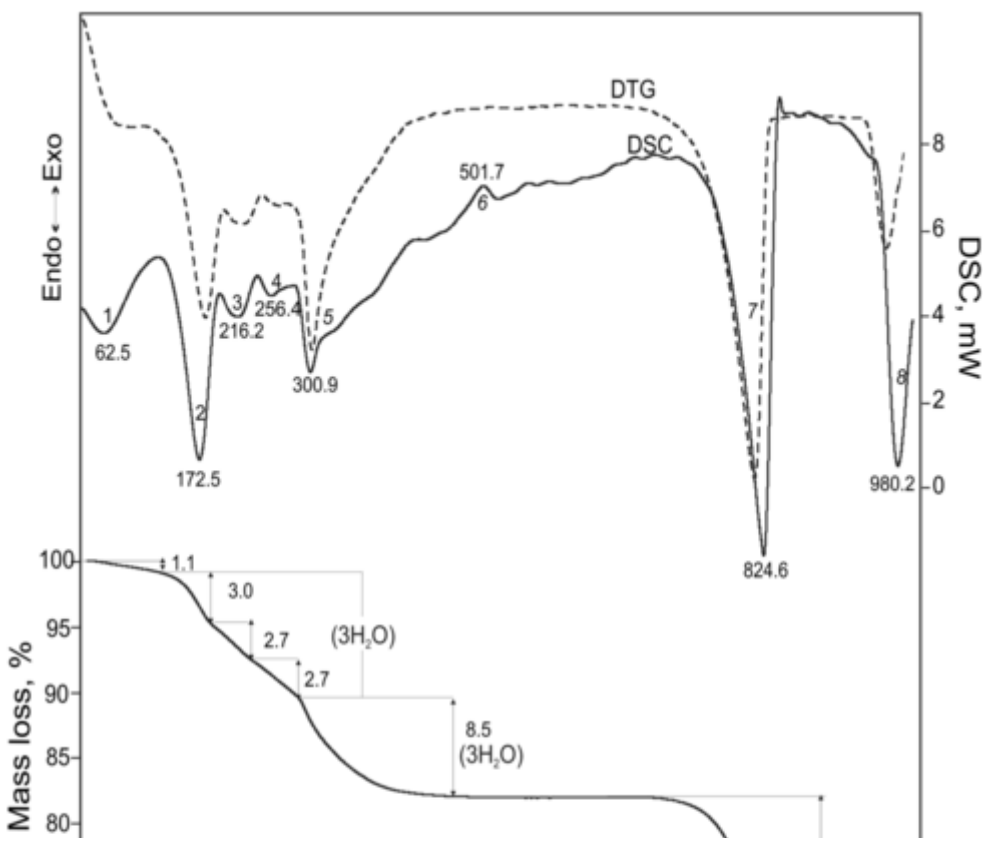

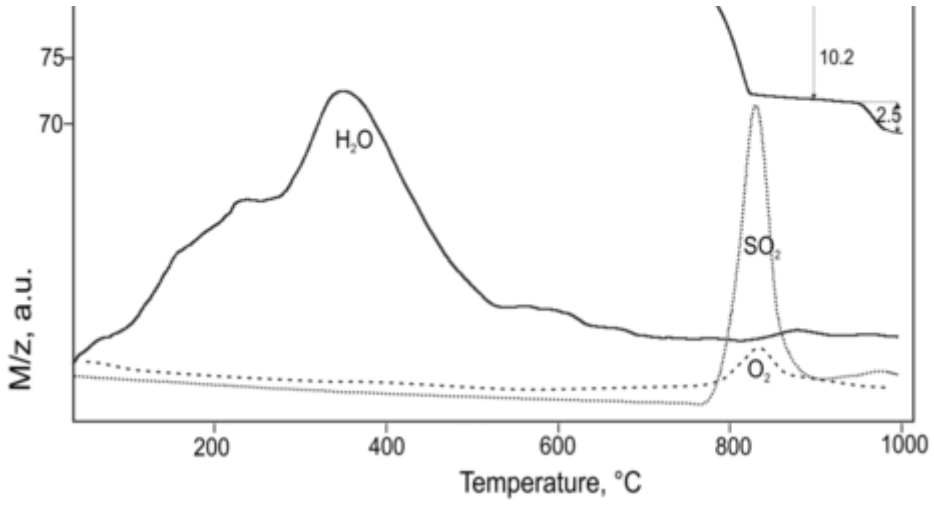

The dehydration process occurs in the low-temperature range (20–280 °C), where four endo-effects on the DSC-curve are observed (Fig. 3. effects *1–4*), suggesting a complex process of dehydration. The MS analysis shows only the liberation of H_2O molecules in this range. The endo-effect *1* reflects the releasing of physisorbed H_2O while the three structural H_2O molecules leave the structure in three clearly distinguishable stages as seen from the TG curve: endo-effects *2–4*. The process of dehydroxylation is observed within endo-effect *5* on the DSC curve in the temperature range 280–500 °C. As can be expected only H_2O is registered by MS. Estimated from the TG curve, three H_2O molecules leave the sample during this process which corresponds well with the six OH groups per formula unit. The observed exothermic effect *6* at 502 °C has been ascribed to the formation of $Cu_2O(SO_4)$ and CuO (Uzunov et al. 1995; Koga et al. 2008) as well as $Zn_3O(SO_4)$ and ZnO (Delcheva et al. 2020). The SO_4 degradation process partially proceeds in the temperature range 780–1000 °C within the endo-effects *7* and *8* on the DSC curve. MS data show the presence of SO_2 and O_2 as evolving gases. According to the TG data, one SO_4 group decomposes in this period. The effect *7* has been attributed to the decomposition of $Cu_2O(SO_4)$ (Koga et al. 2008) followed by the decomposition of $Zn_3O(SO_4)_2$ (endo-effect *8*) (Stanimirova et al. 2016). The remaining amount of SO_2 and O_2 is probably released after 1000 °C due to the decomposition of $CaSO_4$.

The MS analysis in combination with DSC-TG in our study allows a correct determination of the moment of separation for each type of volatile components during heating, as well as the number of H_2O molecules released in different stages. In contrast, the work of Yakhontova et al. (1984), presents only the total mass loss of H_2O and SO_3.

Crystal structure

SZ – The crystal structure of the studied sample was refined in the SG *I*2 and emphasises copper-zinc-centred octahedral layers decorated on both sides by sulfate tetrahedra (Fig. 4 a). The layers have chemical composition $[(Cu_{3.3}Zn_{0.7})(OH)_6(SO_4)_2]^{2-}$ and their negative charge is compensated by calcium ions, situated between the layers and coordinated by oxygen atoms from the sulfate groups and H_2O molecules. There are five symmetrically independent crystallographic positions for the octahedrally coordinated atoms: three of them are occupied by Cu^{2+} (Cu1, Cu3, Cu5); one by Zn^{2+} (Zn2) and one (Cu4/Zn4) is mixed with about 60% Cu^{2+} and 40% Zn^{2+}. The metal–oxygen distances within the octahedra correspond to the described occupancies of the positions, namely: the three (CuO_6) octahedra are strongly influenced by the Jahn–Teller effect and each of them has four short Cu – O distances in the range of 1.92—1.99 Å and two very long ones varying between 2.40—2.49 Å (Table 2). The (ZnO_6) polyhedron has an almost perfect geometry with six distances in the range of 2.10—2.14 Å and O – Zn – O angles of about 90˚. The polyhedron formed around the mixed position has metal–oxygen distances in the range between 2.02 and 2.24 Å. The sulfate groups disorder was noted in the experimental part and is presented on Fig. 5. On the figure symmetrically independent S positions are differently coloured and their occupancy is given. The possibilities of combinations of the arrangement of the tetrahedra are as follows: S11 and S21 (up to 48%) of the layers, S12 and S22 (up to 42%) of the layers, S11 and S22 (up to 42%) of the layers and S12 and S21 (up to 52%) of the layers. Both combinations S12/S21 and S11/S22 suppose that sulfate tetrahedra are inclined in the same direction to the normal of the layer, while in the other two combinations S12/S22 and S11/S21 the tetrahedra will be inclined in opposite directions to each other. The four symmetrically independent sulfate groups exhibit geometrical parameters showing distorted tetrahedra. The S – O bonds vary between 1.35 and 1.60 Å

and have average values as follows: $S11O_4$ – 1.516 Å; $S12O_4$ – 1.453 Å; $S21O_4$ – 1.508 Å and $S22O_4$ – 1.473 Å. The interlayer space is occupied by seven-coordinated calcium atoms:four apical sulfate oxygen atoms (the ones which are not involved in Cu/Zn – O bonding) and three H_2O molecules. The Ca – O bond lengths for Ca1 and Ca2 polyhedra vary between 2.35 – 3.04 Å and 2.28 – 2.65 Å respectively.

Fig. 4

Crystal structure of the studied **a** SZ; **b** SL

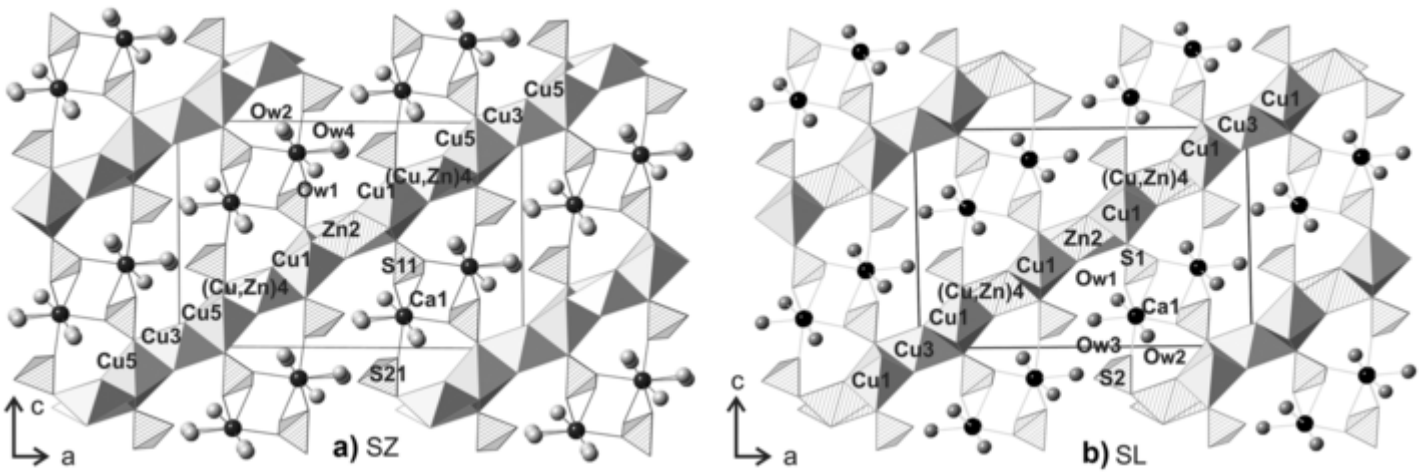

Table 2

Selected bond lengths (Å) for the studied samples

SZ (*I*2)			SL(*I*2/*m*)		
Bond	**Distance (Å)**	**Average distance (Å)**	**Bond**	**Distance (Å)**	**Average distance (Å)**
Cu1–O2	1.964	2.126	Cu1–O1	1.962	2.132
Cu1–O3	1.993		Cu1–O2	1.979	
Cu1–O4	1.954		Cu1–O3	1.979	
Cu1–O5	1.923		Cu1–O4	1.956	
Cu1–O12	2.471		Cu1–O11	2.443	
Cu1–O21	2.451		Cu1–O21	2.475	
Zn2–O2 × 2	2.143	2.127	Zn2–O3 × 4	2.116	2.115
Zn2–O3 × 2	2.133		Zn2–O2 × 2	2.113	
Zn2–O6 × 2	2.104				
Cu3–O3 × 2	1.953	2.133	Cu3–O3 × 4	1.974	2.226
Cu3–O6 × 2	1.974		Cu3–O11 × 2	2.477	
Cu3–O21 × 2	2.472				
(Cu,Zn)4–O1	2.023	2.108	(Cu,Zn)4–O4 × 2	2.043	2.103
(Cu,Zn)4–O1	2.054		(Cu,Zn)4–O4 × 2	2.062	
(Cu,Zn)4–O5	2.023		(Cu,Zn)4–O1	2.199	
(Cu,Zn)4–O5	2.064		(Cu,Zn)4–O21	2.207	
(Cu,Zn)4–O4	2.241				
(Cu,Zn)4–O21	2.242				
Cu5–O1	1.993	2.133			
Cu5–O2	1.984				
Cu5–O4	1.944				
Cu5–O6	1.984				
Cu5–O12	2.492				
Cu5–O21	2.403				

Fig. 5

The octahedral layer of SZ. The S atoms of the symmetrically independent tetrahedra are marked by different colours. The S atoms site occupancy is given in brackets

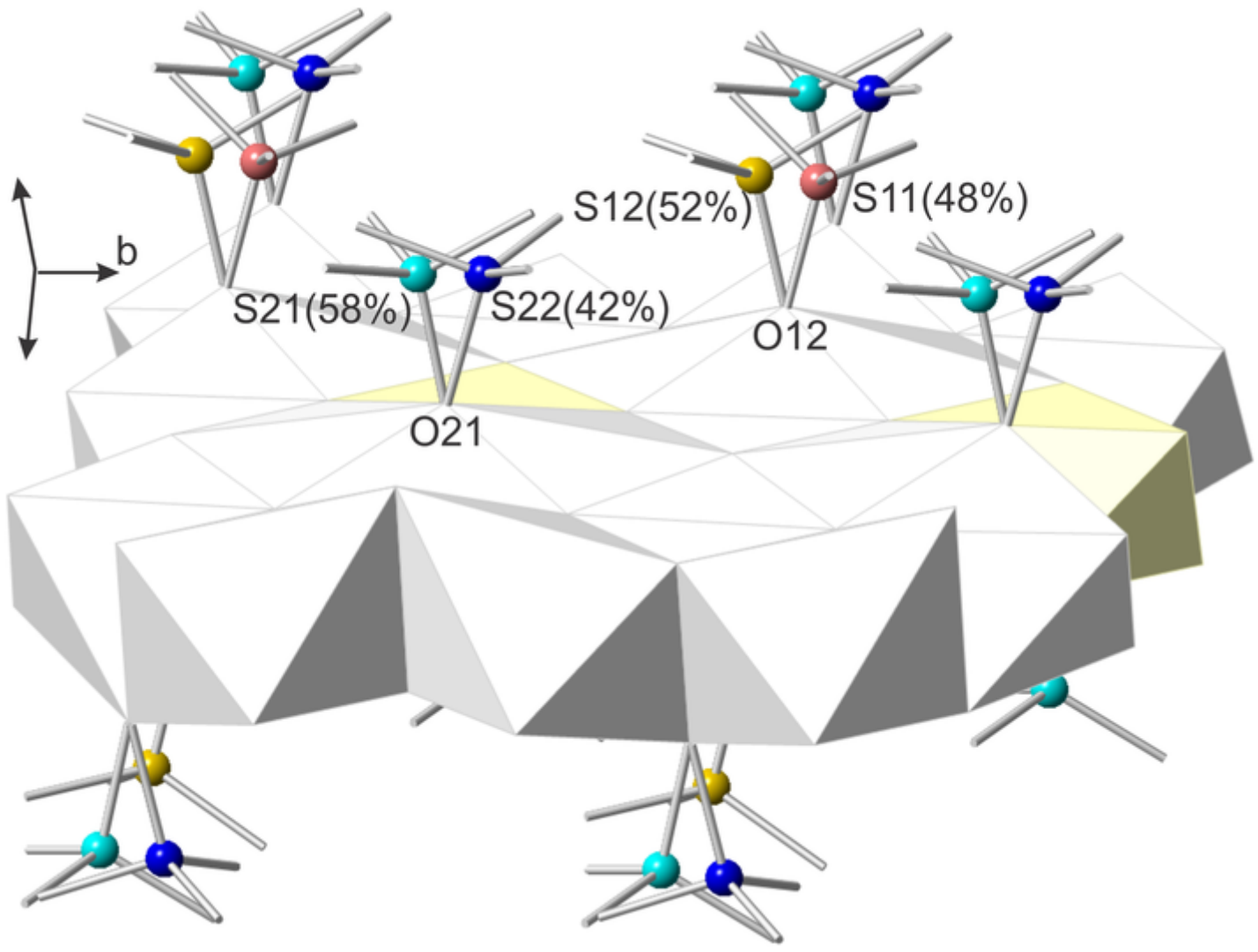

SL – The crystal structure of the studied sample was refined in the *I* 2/*m* SG. It has unit- cell parameters similar to that of the SZ sample (Table 1). The structural topology of SL is similar to that of SZ and contains Cu/Zn octahedral layers interconnected by calcium polyhedra (Fig. 4b). There are two symmetrically independent Cu positions (Cu1, Cu3) one Zn position (Zn2) and one mixed Cu/Zn (Cu4/Zn4) with 27% Cu and 73% Zn. The corresponding metal–oxygen distances are comparable to those found for the SZ and the Cu-centred polyhedra are highly distorted as a consequence of the Jahn–Teller effect while the Zn-centred polyhedron has an almost ideal geometry and in the mixed one (Cu,Zn) – O distances are in the range between 2.04 and 2.21 Å (Table 2). The sulfate tetrahedra are more isometric than those in the SZ structure. The S – O bond lengths vary in the range of 1.46 – 1.52 Å and have average values of 1.47 and 1.48 Å for $S1O_4$ and $S2O_4$ respectively. Three symmetrically independent H_2O molecules and four sulfate oxygens form the Ca-centred polyhedron, where the Ca – O distances are between 2.37 and 3.03 Å. The OW1 oxygen is part of the coordination polyhedra for two adjacent Ca^{2+} ions and forms a strong hydrogen bond with O12 atom from the layer (OW1 ··· O12 = 2.55(1) Å). The OW2 and OW3 molecules are connected to only one Ca atom and are part of a weak hydrogen bonding network (O ··· W2 O4 = 2.86(1) Å and OW3 ··· O23 = 2.76(2) Å). A difference in the binding strength of H_2O molecules is also well illustrated in the DSC-TG curves, commented before: There are three clearly distinguishable effects on the DSC curve (numbers 2, 3 and 4 in Fig. 3), each of them corresponding to the release of one H_2O molecule.

Discussion

The chemical composition of the studied samples corresponds well to that of serpierite, the only difference being the Cu:Zn ratio (Table 3). The studied samples exhibit an architecture based on SO_4 – decorated $[M^{2+}\varphi_2]$ sheets and therefore both SZ and SL have its place among the hydroxy-hydrated copper-sulfate minerals with doubly decorated sheets (Table 4). The structural topology of the minerals listed in Table 4 is presented by means of the schematic presentation used by Pekov et al. (2013). Thus six different types of structural topologies are defined (Figs. 6 and 7). The crystal structures of schulenbergite and minohlite (first two minerals in Table 4) are built of electro-neutral layers and interlayer H_2O molecules. The next structural topology occurs in ktenasite, fehrite and gobelinite with Zn^{2+}, Mg^{2+}, Co^{2+} interlayer cations, respectively. Here the sheets are negatively charged and the interlayer cations are surrounded by H_2O molecules only (Fig. 6a). In the case of campigliaite, the interlayer Mn^{2+} ions are coordinated by four H_2O molecules and two oxygens from two neighbouring sulfate groups (Fig. 6b). Thus, trimers of one interlayer cation and two SO_4 groups,

from the same layer, decorate the octahedral sheets from both sides and layer stacking is achieved in a kind of zip-like mode. The next topology is represented by kobyashevite, christelite and niedermayrite (Cu^{2+}, $Zn^{2+}$and Cd^{2+} interlayer cations respectively). The octahedral sheets are linked through linear trimers, formed by one cation and two SO_4 groups from neighbouring layers (Fig. 6 c). The rest of the minerals in consideration (Table 4.) reveal structural topology where two interlayer cations and four SO_4 groups are linked in a way to form complex $[Cd_2(SO_4)_4]$ groups in edwardsite (Fig. 7 a) or infinite $^{1\infty}[(Ca,Cd)_2(SO_4)_3]$ chains in devilline, serpierite, aldridgeite, SZ and SL (Fig. 7 b). For the last two species lautenthalite and orthoserpierite there is currently no structural information except unit-cell parameters. Among the last group of minerals, serpierite was the first mineral described in the literature, so we use the term "serpierite topology" for the topology presented in Fig. 7 b. Considering the structural peculiarities of SZ and SL, they certainly belong to the minerals with "serpierite topology", for which the following similarities and differences could be defined: i) the translational parameters, describing the octahedral layers are comparable—serpierite (6.25 / 21.85 Å); devilline (6.14 / 22.19 Å); aldridgeite (6.21 / 21.84 Å), SZ(6.22 / 21.89 Å); SL(6.26 / 21.85 Å); ii) the Cu- and Zn-centred octahedra show various types and degrees of deformations and thus each of the studied structures contains layers, which are unique in terms of the number and positions of symmetrically equivalent octahedra; iii) the adjacent infinite chains $^{1\infty}[(Ca/Cd)_2(SO_4)_3]$ connecting the layers also differ depending on the layer stacking and positions of the calcium ions; iv) the three-dimensional stacking of the layers predetermines the size of the third translational parameter and the monoclinic angle, which are: serpierite (22.19 Å / 113.36˚); devilline (20.87 Å / 102.73˚); aldridgeite (22.05 Å / 113.19˚); SZ(18.42 Å / 146.48˚); SL(18.39 Å / 146.39˚); v) in devilline, serpierite and aldridgeite there are two layers per unit cell while in SZ and SL there is only one. According to the mineral nomenclature proposed by IMA Commission (Nickel and Grice 1998), the polytypes differ only in their layer stacking sequences, while "polytypoids are substances that do not fit the strict definition of polytype, and include minerals with the same topology and with somewhat different composition". The SZ and SL samples reveal "serpierite topology" with different stacking sequence of the layers and the layers have somewhat different chemical composition (variable Cu:Zn ratio on individual cation sites). Thus, it could be concluded that SZ and SL samples are serpierite polytypoids and could be designated as serpierite-1 *M*.

Table 3

Reported chemical composition of the serpierite samples

Sample	Chemical formula	Cu:Zn ratio	References
Serpierite, Lavrion	$Ca[(Cu,Zn)_4(SO_4)_2(OH)_6]\bullet 3H_2O$	1.90	Sabelli and Zanazzi (1968)
Aldredgite	$(Ca,Cd)[(Cu,Zn)_4(SO_4)_2\ (OH)_6]\bullet 3H_2O$	2.00	Elliot and Pring (2015)
SL	$Ca[(Cu,Zn)_4\ (SO_4)_2(OH)_6]\bullet 3H_2O$	2.23	this paper
Serpierite Romania	$Ca[(Cu,Zn)_4(SO_4)_2\ (OH)_6]\bullet 3H_2O$	2.80	Zaharia (2003)
SZ	$Ca[(Cu,Zn)_4\ (SO_4)_2(OH)_6]\bullet 3H_2O$	4.71	this paper

Table 4

Hydroxy-hydrated copper-sulfate minerals with doubly decorated sheets

Mineral name	Chemical formula	SG	Unit-cell parameters						References
Schulenbergite	$[(Cu,Zn)_7(OH)_{10}(SO_4)_2]\bullet 3H_2O$	*P* -3	8.211	8.211	7.106	90	90	120	Mumme et al. (1994)
Minohlite	$[(Cu,Zn)_7(OH)_{10}(SO_4)_2]\bullet 8H_2O$	*	8.254	8.254	8.135	90	90	120	Ohnishi et al. (2013)
Ktenasite	$Zn[(Cu,Zn)_4(OH)_6(SO_4)_2]\bullet 6H_2O$	$P2_1/c$	5.589	6.166	23.751	90	95.55	90	Mellini and Merlino (1978)
Fehrite	$Mg[Cu_4(OH)_6(SO_4)_2]\bullet 6H_2O$	$P2_1/c$	5.606	6.129	23.834	90	95.29	90	Schlüter et al. (2021)

*SG missing

Mineral name	Chemical formula	SG	Unit-cell parameters						References
Gobelinite	$Co[Cu_4(OH)_6(SO_4)_2]•6H_2O$	$P2_1/m$	5.599	6.084	23.675	90	95.22	90	Mills et al. (2020)
Campigliaite	$Mn[Cu_4(OH)_6(SO_4)_2]•4H_2O$	$C2$	21.707	6.098	11.245	90	100.3	90	Menchetti and Sabelli (1982)
Kobyashevite	$Cu[Cu_4(OH)_6(SO_4)_2•4H_2O$	P -1	6.064	11.012	5.490	102.58	92.43	92.06	Pekov et al. (2013)
Christelite	$Zn[(Cu,Zn)_4(OH)_6(SO_4)_2]•4H_2O$	P -1	5.414	6.336	10.47	94.32	90.06	90.27	Adiwidjaja et al. (1996)
Niedermayrite	$Cd[Cu_4(OH)_6(SO_4)_2]•4H_2O$	$P2_1/m$	5.543	21.995	6.079	90	92.04	90	Giester et al. (1998)
Edwardsite	$Cd[(Cu,Cd)_4(OH)_6(SO_4)_2]•4H_2O$	$P2_1/c$	10.863	13.129	11.169	90	113.04	90	Elliot et al. (2010)
Aldridgeite	(Cd,Ca) $[(Cu,Zn)_4(OH)_6(SO_4)_2]•3H_2O$	$C2/c$	22.049	6.212	21.832	90	113.19	90	Elliot and Pring (2015)
Devilline	$Ca[Cu_4(OH)_6(SO_4)_2]•3H_2O$	$P2_1/c$	20.870	6.135	22.191	90	102.44	90	Sabelli and Zanazzi (1972)
Dimorph of Devilline	$CaCu_4(SO_4)_2(OH)_6•3H2O$	$P2_1/c$	10.432	6.139	22.213	90	102.76	90	Kolitsch et al. (2013)
Serpierite	$Ca[(Cu,Zn)_4(OH)_6(SO_4)_2]•3H_2O$	$C2/c$	22.186	6.250	21.853	90	113.36	90	Sabelli and Zanazzi (1968)
Orthoserpierite	$Ca[Cu_4(OH)_6(SO_4)_2]•3H_2O$	$Pca2_1$	22.100	6.200	20.390	90	90	90	Sarp (1985)
Lautenthalite	$Pb[Cu_4(OH)_6(SO_4)_2]•3H_2O$	$P2_1/c$	21.624	6.040	22.544	90	108.2	90	Medenbach and Gebert (1993)
SZ – this study	$Ca[Cu_{3.3}Zn_{0.7}(OH)_6(SO_4)_2]•3H_2O$	$I2$	18.418(3)	6.220(1)	12.091(2)	90	90.78(1)	90	this paper
SL – this study	$Ca[Cu_{2.8}Zn_{1.2}(OH)_6(SO_4)_2]•3H_2O$	$I2/m$	18.394(1)	6.256(1)	12.097(1)	90	90.92(1)	90	this paper
*SG missing									

Fig. 6

Schematic presentation of the structural topologies of **a** ktenasite, fehrite and gobelinite; **b** campigliaite; **c** kobyashevite, christelite and niedermayrite

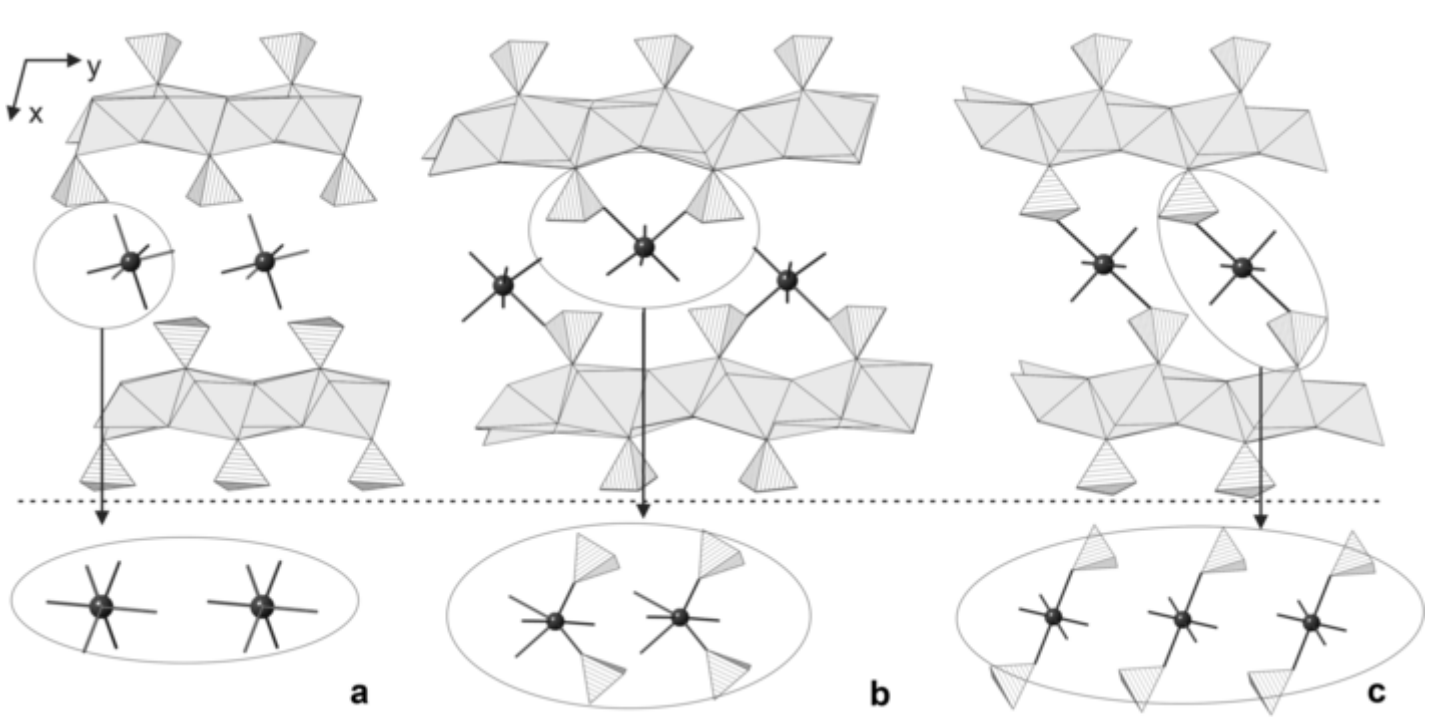

Fig. 7

Schematic presentation of the structural topologies of **a** edwardsite; **b** devilline, serpierite and aldridgeite

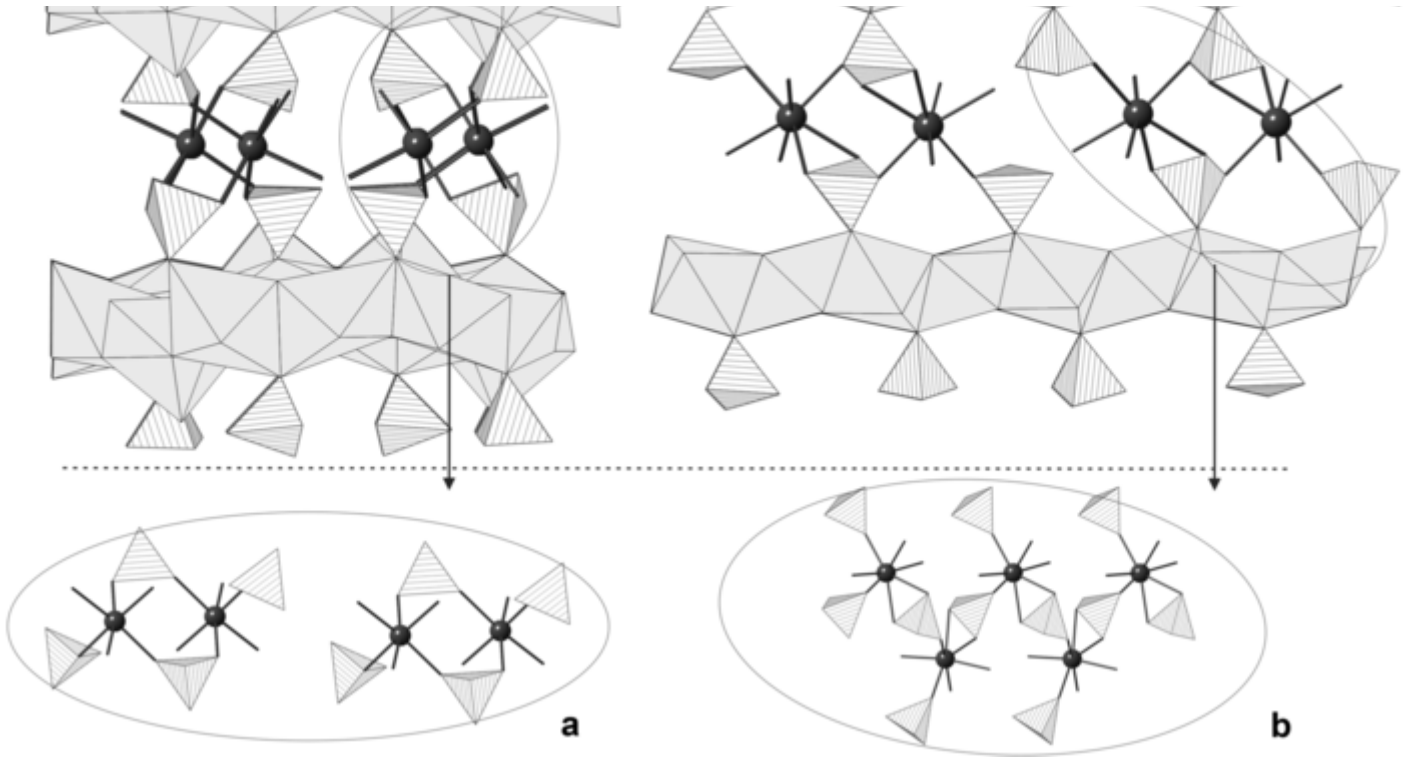

Conclusions

The first find of serpierite in Bulgaria is reported. Samples from the Zvezdel deposit (Bulgaria) and Lavrion (Greece) are studied and their characteristics are compared with those described by Sabelli and Zanazzi (1968). The sample from Zvezdel shows a smaller amount of zinc than that of any serpierite specimen reported until now in the literature. The thermoanalytical data are consistent with the structural data which show the presence of three types of H_2O molecules. The studied samples exhibit crystal structures with “serpierite topology” which is one of the six topologies defined for the hydroxy-hydrated copper sulfate minerals with doubly decorated sheets. All the described topological models suggest a wide range of possible deformations of the octahedral layer, the stacking manner and the interlayer species. Thus, a larger variety of polytypes and polytypoids of the known hydroxy-hydrated copper sulfate minerals could be expected. Both studied samples represent a new polytypoid designated as serpierite-1 *M*.

Publisher's Note

Acknowledgements

This work was supported by the Bulgarian Ministry of Education and Science under the “National Centre for Mechatronics and Clean Technology” (grant agreement BG05M2OP001-1.001-0008).

Author contribution

Rositsa P. Nikolova: Conceptualization, Methodology, Writing original draft, Investigation, Resources, Supervision, Validation, Writing review & editing. Nadia L. Petrova: Methodology, Writing original draft, Data curation, Formal analysis, Visualization, Investigation, Validation. Zlatka G. Delcheva: Resources, Formal analysis. Liliya V. Tsvetanova: Formal analysis, Visualization. Tzveta Stanimirova: Writing review & editing.

Declarations

Competing interest The authors declare that they have no known competing financial interests or personal relationships that could have appeared to influence the work reported in this paper.

Supplementary Information

Below is the link to the electronic supplementary material.

Supplementary file1 (DOCX 6260 KB)

References

Adiwidjaja G, Friese K, Klaska KH, Schlüter J (1996) The crystal structure of christelite $Zn_3Cu_2(SO_4)_2(OH)_6 \bullet 4(H_2O)$. Z Kristallogr 211:518–521

Aroyo MI, Perez-Mato JM, Orobengoa D, Tasci E, de la Flor G, Kirov A (2011) Crystallography online: Bilbao Crystallographic Server. Bul Chem Commun 43(2):183–197

Bertrand E (1881) Étude optique de différents minéraux. Bull Soc Miner France 4:87–89

Bridges TF (1987) Serpierite and devilline from the Northern Pennine Orefield. Proc Yorks Geol Soc 46(2):169–169

Campostrini I, Gramaccioli CM (2001) Selenium-rich secondary minerals from the Baccu Locci mine (Sardinia, Italy). N Jb Miner Abh 177(1):37–59

CrysAlis PRO (2011) Agilent Technologies, UK Ltd, Yarnton, England

Delcheva Z, Tsvetanova Y, Petrova N, Tacheva E, Nikolova R (2017) First data for mineral of devilline group from Zvezdel, Eastern Rhodopes, Bulgaria. Geosciences 2017:19–20

Delcheva Z, Petrova N, Stanimirova TS (2020) Thermal decomposition of ktenasite. Rev Bulg Geol Society 81(3):25–27

Des Cloizeaux M (1881) Étude de différents minéraux. Bull Soc Miner France 4:89–96

Elliot P, Brugger J, Caradoc-Davies T (2010) Description and crystal structure of a new mineral, edwardsite, $Cu_3Cd_2(SO_4)_2(OH)_6 \bullet 4H_2O$, from Broken Hill, New South Wales, Australia. Mineral Mag 74:39–53

Elliott P, Pring A (2015) Aldridgeite, a new mineral from the Block 14 Opencut, Broken Hill, New South Wales. Austral J Mineral 17:67–71

Elliott P, Willis AC (2010) Crystal Chemistry of Cadmium Oxysalt and associated Minerals from Broken Hill, New South Wales. In: Elliott P (PhD Thesis) The University of Adelaide, Crystal structure of cadmian serpierite from the Block 14 Opencut, Broken Hill, New South Wales, pp 65–90

Frenzel A (1895) Mineralogisches Tscherm Mineral Petrog Mitt 14:121–130

Giester G, Rieck B, Brandstätter F (1998) Niedermayrite, $Cu_4Cd(SO_4)_2(OH)_6 \bullet 4H_2O$, a new mineral from the Lavrion Mining District, Greece. Mineral Petrol 63:19–34

Hammarstrom JM, Seal RR, Meierb AL, Kornfeld JM (2005) Secondary sulfate minerals associated with acid drainage in the eastern US: recycling of metals and acidity in surficial environments. Chem Geol 215:407–431

Hawthorne FC, Schindler M (2000) Topological enumeration of decorated $[Cu^{2+}\phi_2]_N$ sheets in hydroxy-hydrated copper oxysalt minerals. Can Mineral 38:751–761

Koga N, Mako K, Kimizu T, Tanaka Y (2008) Thermal decomposition of synthetic antlerite prepared by microwave-assisted hydrothermal method. Thermochim Acta 467:11–19

Kolitsch U, Brandstätter F, Schreiber F, Fink R, Auer C (2013) Die Mineralogie der weltweit einzigartigen Sc hlacken von Waitschach, Kärnten. Ann Naturhistor Mus Wien A (115):19–87

Marchev P, Kaiser-Rohrmeier M, Heinrich Ch, Ovtcharova M, von Quadt A, Raicheva R (2005) Hydrotherma l ore deposits related to post-orogenic extensional magmatism and core complex formation: The Rhodope Mas sif of Bulgaria and Greece. Ore Geol Rev 27(1–4):53–89

Matsubara S (1973) Occurrence of serpierite from the Kurokawa Mine, Gifu Prefecture. Japan Bull Natn Sci Mus Tokyo 16(4):751–755

Medenbach O, Gebert W (1993) Lautenthalite, $PbCu_4[(OH)_6(SO_4)_2]•3H_2O$, the Pb analogue of devillite. A ne w mineral from the Harz mountains. Germany N Jb Miner Monat 9:401–407

Menchetti S, Sabelli C (1982) Campigliaite, $Cu_4Mn(OH)_6(SO_4)_2•4H_2O$, a new mineral from Campiglia Maritt ima, Tuscany, Italy. Amer Miner 67:385–393

Mellini M, Merlino S (1978) Ktenasite, another mineral with $^2{}_\infty[(Cu, Zn)_2(OH)_3O]$- octahedral sheets. Z Kris tallogr 147:129–140

Mills SJ, Kolitsch U, Favreau G, Birch WD, Galea-Clolus V, Henrich JM (2020) Gobelinite, the Co-analogue of ktenasite from Cap Garonne, France, and Eisenzecher Zug, Germany. Eur J Mineral 32:637–644

Moritz R, Márton I, Ortelli M, Marchev P, Voudouris P, Bonev N, Spikings R, Cosca M (2010) A review of ag e constraints of epithermal precious and base metal deposits of the Tertiary Eastern Rhodopes: Coincidence w ith Late Eocene-Early Oligocene tectonic plate reorganization along the Tethys. Proc XIX CBGA Congress, T hessaloniki, Greece 100:351–358

Mumme WG, Sarp H, Chiappero PJ (1994) A note on the crystal structure of schulenbergite. Arch Sci Geneve 47:117–124

Nickel EH (1998) Grice JD (1998) The IMA Commission on New Minerals and Mineral Names: procedures a nd guidelines on mineral nomenclature. Mineral Petrol 64(1):237–263

Ohnishi M, Kobayashi S, Kusachi I (2002) Ktenasite from the Hiaro mine at Minoo, Osaka, Japan. J Mineral Petrol Sci 97:185–189

Ohnishi M, Shimobayashi N, Nishio-Hamane D, Shinoda K, Momma K, Ikeda T (2013) Minohlite, a new cop per-zinc sulfate mineral from Minoh, Osaka. Japan Mineral Mag 77(3):335–342

Ohnishi M, Kusachi I, Kobayashi S, Yamakava J (2007) Mineral chemistry of schulenbergite an it's Zn-domin ant analogue from the Hiaro mine at Minoo, Osaka, Japan. J Mineral Petrol Sci 102:233–239

Ohnishi M, Kobayashi S, Kusachi I, Yamakava J, Shirakami M (2004) Ramsbeckite from the Hiaro mine at M inoo, Osaka, Japan. J Mineral Petrol Sci 99:19–24

Pekov IV, Zubkova NV, Yapaskurt VO, Belakovskiy DI, Chukanov NV, Kasatkin AV, Kuznetsov AM, Pushch arovsky DY (2013) Kobyashevite, $Cu_5(SO_4)_2(OH)_6•4H_2O$, a new devilline-group mineral from the Vishnevye Mountains, South Urals, Russia. Mineral Petrol 107:201–210

Sabelli C, Zanazzi PF (1968) The crystal structure of serpierite. Acta Cryst B24:1214–1221

Sabelli C, Zanazzi PF (1972) The crystal structure of devillite. Acta Cryst B28:1182–1189

Sarp H (1985) Orthoserpiérite $Ca(CuZn)_4(SO_4)_2(OH)_6•3H_2O$, un nouveau minéral de la Mine de Chessy, France, polymorphe de la serpiérite. Schweiz Mineral Petrog Mitt 65:1–7

Schlüter J, Malcherek T, Mihailova B, Rewitzer C, Hochleitner R, Müller D, Günther A (2021) $MgCu_4(SO_4)_2(OH)_6•6H_2O$, the magnesium analogue of ktenasite from the Casualidad mine near Baños de Alhamilla, Almeria, Spain. N Jb Miner Abh 197:1–10

Sheldrick G (2015) Crystal Structure Refinement with SHELXL Acta Cryst C71:3–8

Sheldrick G (2008) A short history of *SHELX*. Acta Cryst A64:112–122

Staminirova T, Petrova N, Kirov G (2016) Thermal decomposition of zinc hydroxy-sulfate-hydrate minerals. J Therm Anal Calorim 1:85–96

Takada M, Matsuuchi S (1981) Secondary minerals from the Kabasaka mine and Nyukaku mine, Hyogo Prefecture (Japan) - serpierite, devilline, langite, spangolite, and woodwardite. Chigaku Kenkyu 32:191–199

Uzunov I, Klissurski D, Teocharov L (1995) Thermal decomposition of basic copper sulfate monohydrate. J Therm Anal 44(3):685–696

Van Tassel R (1979) Minéraux artificiels ou de néoformation à Plombières et Sclaigneau. Belgique Bull Soc Belg Geol 88:273–279

Yakhontova LK, Postnikova VP, Vlasova EV, Sergeeva NE (1981) New data on posnjakite, serpierite and woodwardite. Dokl Akad Nauk SSSR 256:1221–1225

Yakhontova LK, Postnikova VP, Sergeeva NE, Yudin RN (1984) New data on rare copper sulfates. Moscow Univ Geol Bull 39(3):41–46

Zaharia L (2003) Serpierite Ca(Cu, $Zn_)4(OH_)6(S_O4_)2•3_H2O$ - the first occurrence in Romania. Studia UBB Geologia 48(1):77–84